RESEARCH ARTICLE Journal of Daylighting 11 (2024) 372-390 doi:10.15627/jd.2024.25

ISSN 2383-8701

Journal of Daylighting

Journal homepage: https://solarlits.com/jd

# Optimum Geometry of Double-skin Self-Shading Facade of Classrooms with the Aim of Creating Energy Saving and Visual Comfort in Isfahan Province, Iran

Shirin Aghamohammadiha, Narges Dehghan*

*Department of Architecture, Advancement in Architecture and Urban Planning Research Center, Najafabad Branch, Islamic Azad University, Najafabad, Iran*

**Article info**

***Article history:***
Received 15 July 2024
Revised 4 September 2024
Accepted 21 September 2024
Published online 19 November 2024

***Keywords:***
Double-skin self-shading façade
Visual comfort
Geometry
Classroom

**Abstract**

The significant energy consumption in educational spaces worldwide and its environmental impact greatly influence the quality of space, learning levels, and student comfort. Despite offering free school energy costs, developing countries like Iran have not established specific design principles to ensure student comfort. Additionally, the poor design of school building exteriors, such as the common installation of large, unshaded windows in Iranian schools, causes glare issues. The primary objective of this study is to control direct sunlight and increase shading, thereby reducing its impact on energy consumption and enhancing visual comfort. This paper proposes a novel solution that combines a self-shading facade with a double-skin facade for classroom spaces. The study variables, involving the modification of the geometry of the double-skin self-shading facade via DesignBuilder software and the Daysim plugin, were compared to a simple double-layer facade. Based on the results, the optimal scenario for the self-shading double-skin façade with the specifications of a triangular pyramid module shape, ridge position fold 3/2 the module height, cavity depth 7.0, and number of module 2×2 exhibited 40% lower cooling load, 25% lower heating load, and 95% lower lighting load than a simple double-skin facade. At the same time, all scenarios of the new solution provided better visual comfort and daylighting criteria compared to the simple double-skin facade. The modularity and use of indigenous brick materials in the double-skin self-shading facade design reduce construction costs.

© 2024 The Author(s). Published by solarlits.com. This is an open access article under the CC BY license (https://creativecommons.org/licenses/by/4.0/).

## 1. Introduction

One factor contributing to increased energy consumption is the impact of direct and diffuse solar radiation in urban areas. This phenomenon, known as the urban heat island effect, raises temperatures locally, regionally, and globally [1]. Global energy consumption in buildings is projected to rise by an average of 5.1% annually between 2012 and 2040, primarily for cooling, heating, lighting, and appliances [2]. Schools are significant energy consumers, comparable to residential and office buildings [3]. In Iran, the average energy consumption in schools, the most numerous type of public building, exceeds 160 kWh/m² [4]. This is 5.2 times higher than the annual consumption of schools in developed countries, around 65 kWh/m² [5]. Iranian schools receive partial exemptions from energy costs under a Ministry of Education directive.

Four key passive design elements reduce direct solar radiation, increase shading, and decrease energy consumption: self-shading facades (FSS), shading devices (SD), the window-to-wall ratio (WWR), and building orientation (BO) [6]. Self-shading methods are crucial in hot climates, as they block and control direct sunlight, reducing cooling loads [7,9]. Numerous studies since the 1960s have shown a strong link between classroom temperature, air quality, student performance and comfort [10-12].Another passive strategy to manage heat gain in warm seasons, heat loss in cold seasons, and thermal discomfort from uneven solar radiation is the double-skin facade (DSF). The DSF consists of two layers of glass with a ventilated air cavity acting as a thermal buffer. DSFs also play a vital role in controlling glare and maximizing daylight through correctly placing shading devices [13]. Despite schools in Iran's hot and dry regions consuming 9.41% of total energy, no specific guidelines or codes exist for their design [14].

*Corresponding author.
shirin.aghamohammadi.aim@gmail.com (S. Aghamohammadiha)
dehghan@par.iaun.ac.ir (N. Dehghan)

2383-8701/© 2024 The Author(s). Published by solarlits.com. This is an open access article under the CC BY license (https://creativecommons.org/licenses/by/4.0/).

**Nomenclature**

| | |
|---|---|
| *FSS* | *self-shading facades* |
| *SD* | *shading devices* |
| *WWR* | *window-to-wall ratio* |
| *BO* | *building orientation* |
| *DSF* | *double-skin facade* |
| *U-Value* | *U-Value is the unit of measurement used to assess heat transmittance through materials, including walls, floors, ceilings, and each pane of glass.* |
| *HVAC* | *is an acronym that stands for Heating, Ventilation, and Air Conditioning* |
| *DA* | *Daylight Autonomy* |
| *DGP* | *Daylight Glare Probability* |
| *DF* | *Daylight Factor* |
| *SDA* | *Spatial Daylight Autonomy* |
| *ASE* | *Annual Sunlight Exposure* |
| *UDI* | *Useful Daylight Illuminance* |
| *BWk* | *Cold desert climate* |

Researchers have explored various solutions for school buildings, including self-shading volumes, facade bricklaying patterns, fixed and movable self-shading shapes, complex photovoltaic panel modules, and curved origami lines [15-37]. These approaches aim to improve thermal and visual comfort near windows, reduce cooling loads, enhance indoor light quality, and lower lighting energy consumption.

Standard passive design methods for thermal and visual comfort in schools involve combining window-to-wall ratios with shading devices, optimal orientation, louvers, blinds, and high shading coefficient glass [38-42]. They also utilize light shelves and reflectors [43-46] and consider the effects of sloping walls, orientation, window-to-wall ratio, and glass light transmittance in hot and dry climates [47]. In tropical climates, internal reflections from the ceiling, floor, and walls are employed [48]. A high-performance building facade design results in appropriate daylighting, increased use of daylight to improve student performance, and enhanced comfort [49]. Shading systems are one of designers' most popular strategies to improve facade performance [50]. These systems protect buildings from direct sunlight [51,52] and control daylight penetration [52-54]. Self-shading is a defining feature of appropriate daylighting for schools in tropical [48] and hot, dry climates [47]. The decrease in the surface temperature of the single-paned glass during the winter causes cold radiation to the occupants, while the need for heating and lighting is eliminated by double-skin the facade and increasing the U-Value and maintaining the ambient heat. However, doubling the facade increases cooling loads and decreases heating loads [55]. The most effective strategy to mitigate cooling loads is external shading devices and ventilating the cavity between the skins[56,57]. Minimum heating loads can be achieved by combining a double-skin box structure with external shading [58]. The cavity reduces the U-value of external surfaces and can be used for ventilation and preheating the interior, thus lowering heating loads. The high thermal mass of a brick facade helps stabilize the DSF cavity air temperature, reducing it during periods of intense solar radiation [59]. As schools generally require high fire and noise protection, DSFs act as barriers, preventing the spread of fire, smoke, and noise to adjacent classrooms [13-60].

Given the importance of constructing new schools and improving existing ones in Iran, this research proposes a novel solution for school building facades. It combines a modular self-shading facade with a brick double-skin facade. The form and number of self-shading modules control direct sunlight while allowing adequate light, reducing cooling loads and lighting consumption, and creating visual comfort in classrooms. The double-skin box structure, combined with external shading, offers the benefits of double-skin facades while reducing heating loads. The cavity double-skin facade and depth of the self-shading modules help lower the U-value of external surfaces, facilitate ventilation, and preheat the interior. This allows areas near windows to be used in winter despite cold radiation, while the double-skin protects against fire and noise. Due to the high thermal mass of brick, the brick and glass facade positively impacts the double-skin cavity air temperature.

## 2. Literature review

Buildings with poorly designed facades exposed to direct sunlight rapidly increase the surface temperature and cooling load. In contrast, well-designed buildings, aside from controlling solar radiation impacts, can slow down this heat transfer, thus reducing internal energy demands, which results in energy savings for HVAC systems [61,62]. Self-shading volumes may have inverted pyramid shapes or inward-facing terraces [15-20], and the more a form's surface is inclined towards solar radiation, the greater the cooling capacity in terms of the surface-to-volume ratio [18-21]. Studies on the thermal performance of shading, such as bricklaying textures [7-22], self-shading facade shapes and forms[24-26], patterned facade geometric designs [23-27], and complex fixed modules with concave and convex edges [32,33] as fixed and modular shading demonstrated that they could scatter direct sunlight, improve indoor light quality, and reduce lighting consumption [26]. Parametric movable designs with facade module rotations and shifts [31] and the opening and closing of these structures are incredibly efficient in controlling direct sunlight and dynamic daylight [28-34] and can reach target brightness levels without glare [25]. Prismatic shapes [30], movable louvers [63], and curved origami lines 34 can change based on dynamic daylight and user position, leading to visual comfort. Another passive design solution is installing energy storage devices on the sloped double-skin facade, utilizing direct sunlight [64]. Although deviation from the orthogonal facade increases the heating load, it is balanced by reducing the cooling load and increasing energy production from photovoltaic panels [35-37]. DSFs have been studied recently to improve energy performance while maintaining thermal and visual comfort [65]. DSFs are classified based on the system structure or how the intermediate cavity is divided [13]. The lowest temperature and minimum heating and cooling loads can be achieved by ventilating the cavity and shading the external box structure of the double-skin facade [57,58]. Besides energy efficiency, the double-skin facade increases comfort, raises the thermal resistance of the external wall, and reduces heat loss in winter [9]. Narrower cavities provide a more pronounced chimney effect and better air movement, leading to more efficient extraction of warm air. The cavity depth of the double-skin system, between 0.7 and 1.2 meters, is recommended [66]. Using glass with a higher light

2383-8701/© 2024 The Author(s). Published by solarlits.com. This is an open access article under the CC BY license (https://creativecommons.org/licenses/by/4.0/).

transmission coefficient in the outer layer (single glazing instead of double glazing) raises the cavity temperature, allowing for suitable natural ventilation. On the other hand, double-glazed glass with high thermal insulation is likely used in the inner facade layer due to reduced heat transfer from its conductive and radiative components across the façade [67,68]. Consequently, the performance of DSFs is highly dependent on the facade geometry due to the physics of heat transfer processes occurring within the cavity [56-69]. Indoor environmental conditions in educational infrastructure are closely related to buildings' architectural features and structure, and external shading is one such solution [70]. Installing external shading devices and improving visual comfort minimizes curtain use [71]. Various types of horizontal, vertical, and egg-crate shading are used in hot regions [72], and the length, number, and slope angle of the wall are crucial for controlling solar radiation [71-73]. Daylight design optimization using self-shading in classrooms showed that the sloped wall opening plays a significant role in controlling sunlight inside the room [48]. Sloped building facades with more windows exhibit lower Daylight Autonomy (DA) and Daylight Glare Probability (DGP) values, with the wall slope angle influencing DA levels [47]. As noted, poor facade design in a flat configuration without passive solutions in hot and dry climates leads to increased direct solar radiation and, consequently, higher energy consumption. Two strategies were considered to address this: self-shading facades and double-skin facades.

**Table 1.** Summarize the research background.

| Name/Year | Climate | Usage | Solution | Independent Variable | Dependent Variable | Module Image & software | Results |
|---|---|---|---|---|---|---|---|
| [55] | Semi-warm and humid | Office | A vertical blind inside double-skin with an open window | Shade location inside the double-skin | Energy consumption | 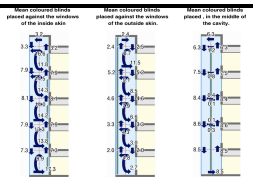 | • Proper impact of shade position and color on the temperature of double-skin windows, reduced cooling load |
| [26] | Hot | | Fixed self-shading | Form and Geometry | Energy saving | Ecotect | •Reduced heat and increased shading |
| [24] | Hot and dry | University | Fixed self-shading | Form and geometry, facade | Energy saving | Design builder 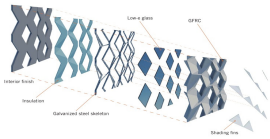 | • 82% reduction in solar heat |
| [25] | Hot | Theater | Fixed self-shading | Form and geometry, direction | Visual Comfort | Diva 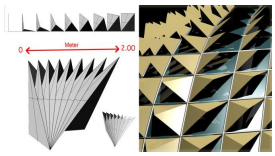 | • Best performance of 1.75-2.00-meter shading slope |
| [23] | | | Fixed patterned facade | Form and Geometry | Thermal performance | Ladybugs, Diva Geco | • Proper performance of horizontal pattern with 180-degree rotation |
| [18] | Hot | Residential | Sloped wall | Slope and geometry | Energy saving | Design builder 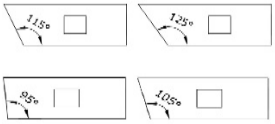 | • Internal heat reduction with a 115-degree facade slope |

2383-8701/© 2024 The Author(s). Published by solarlits.com. This is an open access article under the CC BY license (https://creativecommons.org/licenses/by/4.0/).

| | | | | | | | |
|---|---|---|---|---|---|---|---|
| [44] | Non-Tropical | School | -Light shelves<br>-Light shelves + lower blinds<br>-Upper blinds<br>-Light shelves southern skylight | Roof glazing ration, Light shelf, Horizontal shading | Visual Comfort Energy consumption | 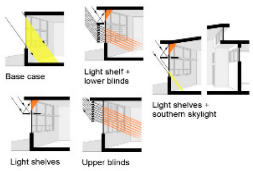 | • cities of Iquique and Santiago: best performance an upper blind<br>• city of Coyhaique, light shelf and southern skylight are good |
| [42] | Non-Tropical | School | movable shading devices | Orientation, Room's depth, WWR, Blind, Internal reflectance, Glass transmittance Context | Visual Comfort | | • window cleaning, proper operation of movable shading devices, painting of interior surfaces with light color to increase the diffuse reflectance of light |
| [46] | Non-Tropical | School | -Light shelves<br>-Blind | Room's depth, WWR, Blind, Occupancy | Visual Comfort | 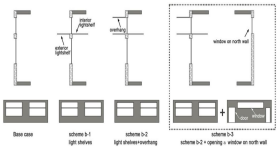 | •light shelves + overhang performs better than other strategies. |
| [21] | Hot and humid | | Self-shading volume | Form and Geometry | Energy saving | Ecotect<br> 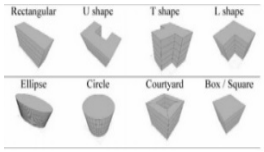 | • Low cooling load with low surface-to-volume ratio |
| [35] | Cold | Office | Energy PV production and double-skin facade | Form and Geometry | Energy consumption | Grasshopper, EnergyPlus<br> 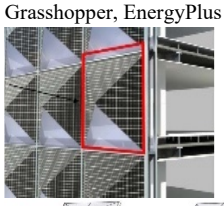 | • Increased heating load, reduced cooling load, increased energy production |
| [9] | Semi-warm and humid | Office | Energy PV production and double-skin facade | Different slope angles | Visual comfort, Energy consumption | 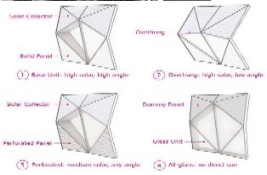 | • Reduced cooling and heating load, artificial lighting use, increased energy production |
| [32,33] | Hot and cold | Office | Energy PV production and fixed shading | Form and Geometry | Visual comfort, Thermal performance | Radiance, EnergyPlus, Ladybug Honeybee<br> 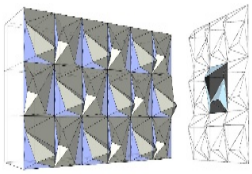 | • Proper form performance for power generation and UDI near the window |
| [10] | Semi-warm and humid | Office | Energy PV production | Form and geometry, facade | Visual comfort, | DIVA-ARCHSIM<br> 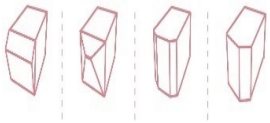 | • Proper performance of shading and energy production |
| [22] | Hot and dry | | Bricklaying | Bricklaying texture | Energy saving | DIVA ArchSim<br> 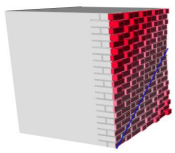 | • Proper performance of 60% protrusion of Finnish brick wall area |
| [36] | Cold | Residential | Energy PV production and double-skin facade | Form and geometry, facade | Energy consumption | EnergyPlus<br> 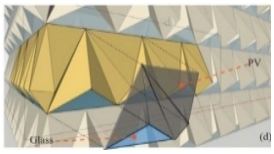 | • Increased heating load, reduced cooling load, increased energy production |

| | | | | | | | |
|---|---|---|---|---|---|---|---|
| [58] | Hot and dry | Office | Double-skin facade | Types of double-skin, | Energy consumption | EnergyPlus 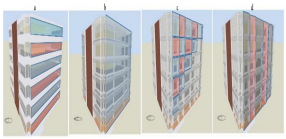 | • Minimum heating load with box model and 30-degree external louver shade |
| [17] | Hot and humid | Office | Sloped wall | Slope angles | Energy saving | ApacheSim 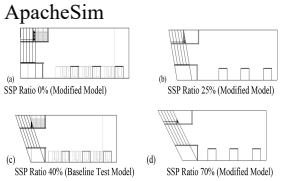  | • Best performance at a 65-degree angle to the horizontal plane |
| [47] | Hot and dry | School | Sloped wall | Different slope angles of the shading facade | Visual comfort, Thermal comfort, Energy consumption | Ladybug Honeybee, Grasshopper 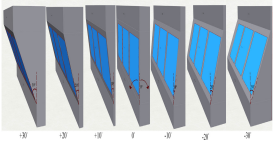 | • Reduced cooling and heating load, artificial lighting use |
| [7] | Hot and dry | | Bricklaying | Texture and facade | Energy saving | Design builder 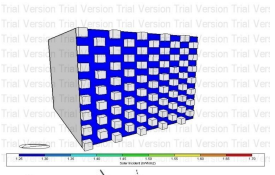 | • Proper performance of horizontal protruding bricks |
| [45] | Non-Tropical | School | -Light shelves -Skylight -tray -Central | WWR, Roof glazing ratio, Light shelf, Blind, Internal reflectance, Shading reflectance, Glass transmittance | Visual Comfort | 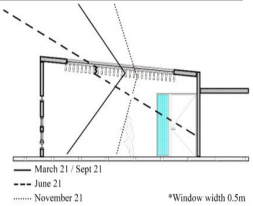  | • central spotlighting + higher reflection indexes provided the best lighting performance |
| [43] | Non-Tropical | School | Light Shelf in Corridor Ceiling | WWR, Light shelf, Wall cavity, Anedolic | Visual Comfort | 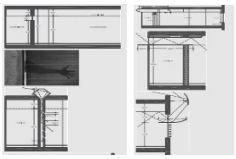 | •Light shelf and rear windows showed the best results as the uniformity level improved and illuminance level increased by average of more than 100%. |
| [48] | Hot and humid | School | Sloped wall | Different slope angles | Visual Comfort | Radiance 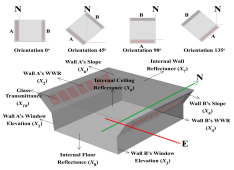 | • Proper performance of the wall with a positive slope in shading and blocking sunlight |
| [59] | Hot, Cold | School | Roof ventilation with double-skin facade and reconstruction | Materials, direction, double-skin opening | Thermal comfort | 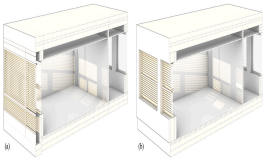 | • Double-skin brick facade reduces cavity air temperature in summer |

A review of existing research on self-shading and double-skin facades reveals that most proposed self-shading solutions focus on volume and wall slopes. Studies on modular facade forms and geometry primarily involve integration with photovoltaic panels, with few solutions exploring repetitive altered fixed module forms. Notably, the concept of a self-shading module as a brick shade for a box-type double-skin facade and its positive impacts on the double-skin cavity and interior space hase not been thoroughly investigated. To address this gap, this research proposes a novel solution combining the modular self-shading form with a brick double-skin facade. The study compares this combined strategy with a flat facade and evaluates its impact on energy consumption and visual comfort in classrooms within the hot and dry climate of Isfahan (Table 1).

2383-8701/© 2024 The Author(s). Published by solarlits.com. This is an open access article under the CC BY license (https://creativecommons.org/licenses/by/4.0/).

## 3. Research methodology

The research approach in this article is quantitative, and the type is simulation. The software DesignBuilder version 7 was used to analyze energy consumption, and for visual comfort analysis and its associated daylight criteria, the Daysim plugin in Rhino software was used. The dependent variables, along with the software programs used to extract them, are shown in the Fig. 1.

### *3.1. Daylighting performance metrics*

The latitude and longitude of Isfahan are 38.32° and 51.4°, respectively, and its elevation above sea level is 1575 meters. The Köppen classification of this city is BSk [74]. Based on long-term statistical studies (1951-2015), the annual average temperature at the Isfahan station is 16.4°C. The average temperature in the coldest month, January, is 3°C, and in the hottest month, July, it is 29.5°C. The total annual hours of sunshine recorded at the Isfahan station is 3274 hours (Isfahan station meteorological data). The DesignBuilder simulation schedule was set from 8 a.m. to 3 p.m. for the entire year, according to the occupancy hours of educational buildings in Iran. To measure visual comfort in the Daysim plugin, the simulation time was set at 12 p.m. on June 21st (the summer solstice).

### *3.2. Research process*

In the first stage, the information databases Google Scholar, Scopus, and ScienceDirect were used to collect related articles. According to the Iranian School Renovation publication, the base classroom model dimensions were set. In line with the research objective and considering the advantages of the two passive solutions (self-shading and double-skin facades) and the identified gaps in the form and geometry of the self-shading modules as external shading of the double-skin facade, the independent and

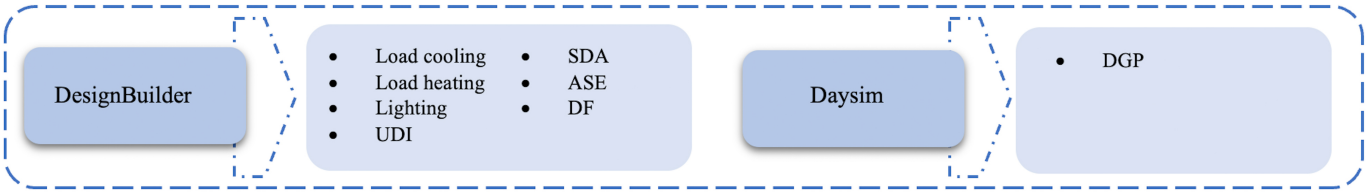


**Fig. 1.** Showing dependent variables.

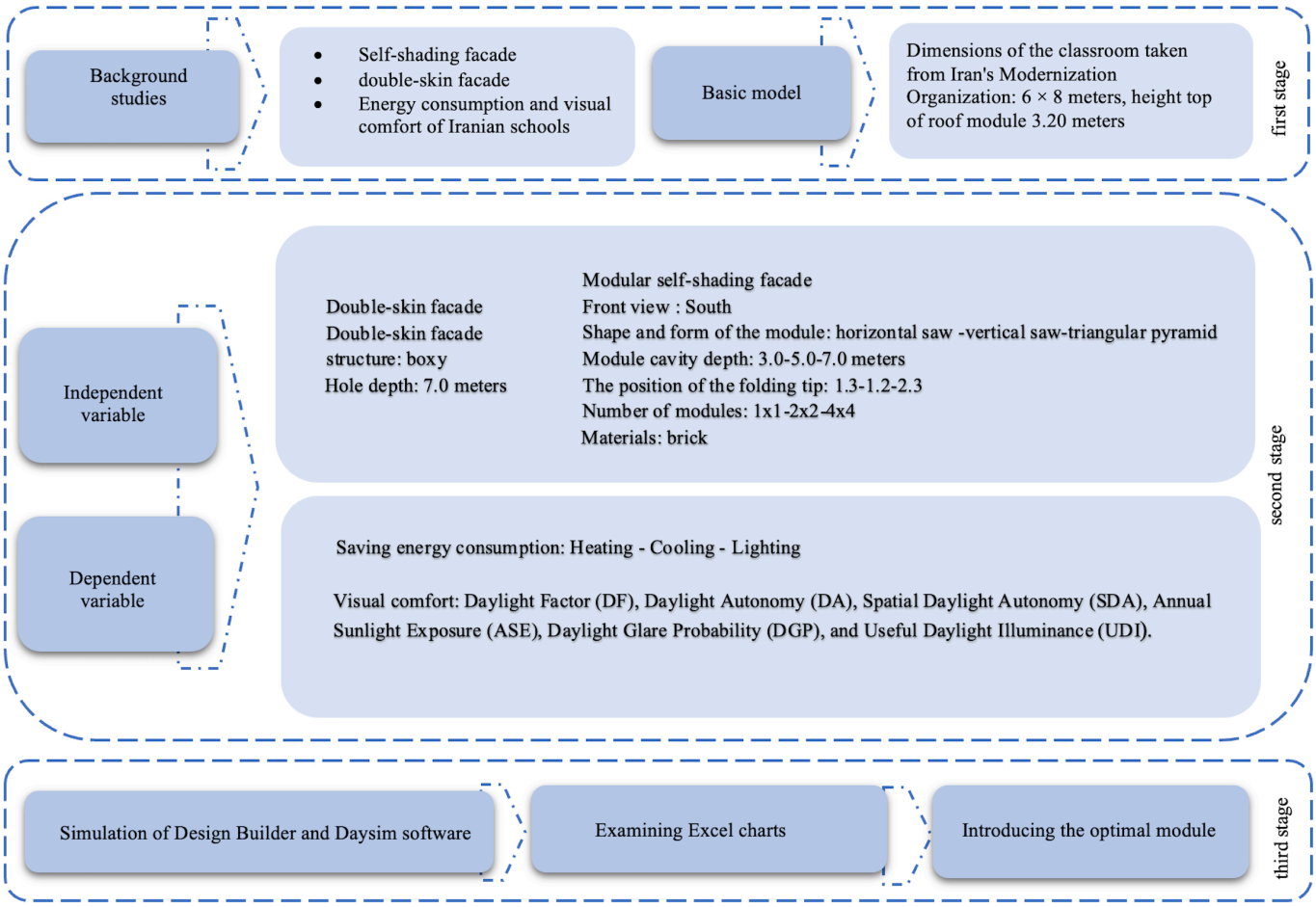


**Fig. 2.** Illustrating research process.

2383-8701/© 2024 The Author(s). Published by solarlits.com. This is an open access article under the CC BY license (https://creativecommons.org/licenses/by/4.0/).

dependent variables were determined. Finally, 81 modules were simulated on the base model using DesignBuilder software to measure energy consumption, and the Daysim plugin in Rhino software was used to measure visual comfort. Detailed explanations regarding the selection and specifics of independent and dependent variables, as well as the creation of simulation process modules, have been provided in the following sections. The optimal module will be identified by analyzing the simulation software's output charts (Fig. 2 shows the research process).

## 4. Materials and methods

### *4.1. Introduction to the base model*

The internal dimensions of the base model for the classroom facade are 8 meters in length, 6 meters in width, and 3.20 top of roof meters in height, set according to the educational building design guidelines [75]. The south-facing facade is 100% glass, with a 100% openable sliding window, and the external walls are uninsulated. The overall settings of the base model are shown in Table 2.

### *4.2. Introduction to research variables*

#### *4.2.1. Independent variables of the flat facade*

The flat facade includes single-pane glass and brick sections for the outer skin, with the entire inner skin composed of double-pane glass. The cavity depth of the flat double-skin facade, recommended by Radhi and colleagues [66], is between 0.7 and 1.2 meters. Therefore, a cavity depth of 0.7 centimeters was considered to ease assembly and facade construction costs. A combination of brick and glass was designed for the southern facade to resemble a self-shading double-skin facade. Structurally, the double-skin facade is of the box type, where airflow inside the cavity occurs through open natural convection [76]. Figure 1 shows the structure, and the details of the inner and outer skins are described in Table 3.

#### *4.2.2. Independent variables of the double-skin self-shading façade*

The independent variables are based on four main parameters: shape, ridge fold position, number of modules, and cavity depth. The window-to-wall ratio of the inner and outer skins, the percentage of openings, the box-type double-skin structure, and the 0.7-meter double-skin depth were considered constant for classroom simulation calculations. Finally, 81 modules enter the simulation process. The simplest folding plate geometry, henceforth called "saw-tooth", consists of a single fold, a module the plate on one side of which consists of glazing and the plate on the side is a brick .A module with horizontal saw-tooth in which the fold is horizontal and vertical saw-tooth in which the fold is vertical. More complex pyramid-based module is a triangular pyramid with a glazing sloped face facing downward. In terms of shading, the horizontal saw-tooth module works best for the

**Table 2.** Base model settings.

| Parameter | Setting |
|---|---|
| Type of Activity | Educational Space |
| Occupancy Density (persons/m²) | 0.4 |
| Schedule | 8:00 - 15:00 |
| Activity | Sitting and walking |
| Winter and Summer Clothing (clo) | Winter: 1.2, Summer: 0.71 |
| Heating System Setpoint (°C) | Heating: 18°, Setback Heating: 12° |
| Cooling System Setpoint (°C) | Cooling: 23°, Setback Cooling: 28° |
| HVAC Type | Chiller with fan coil (four-pipe) |
| Heating COP | 0.85 |
| Cooling COP | 1.8 |
| Classroom Lighting Intensity | 300 Lux |
| Window Model | Single-pane glass, no shading, clear |
| Glass Type | 6 mm clear glass |

**Table 3.** Flat double-skin facade settings (configurations).

| Skins flat double-skin façade | Cavity depth between double-layer | WWR% | Glass opening percentage |
|---|---|---|---|
| inner skin | 0/7 | 100 | 100 |
| outer skin | | 50 | 50 |

**Table 4.** Double-skin self-shading facade settings (configurations).

| Skins double-skin self-shading façade | Cavity depth between double-skin | WWR% | Glass opening percentage | Direction facade | Shape double-skin |
|---|---|---|---|---|---|
| inner skin | 0/7 | 100 | 100 | south | Box |
| outer skin | | 34-65 | 50 | | |

2383-8701/© 2024 The Author(s). Published by solarlits.com. This is an open access article under the CC BY license (https://creativecommons.org/licenses/by/4.0/).

southern facade, and the effect of the vertical saw-toothed module is suitable for the eastern and western facades. The geometry of the folded panel involves two main parameters: the position of the ridge fold or peak of the folded module relative to its edges, the panels' tilt angle, and the module's cavity depth. The ridge position of the module relative to the floor panel was considered, and the glass position was determined. The tilt angle indicates the cavity depth, the angle between the panel ridge and the wall, with the cavity depth minimizing near the module edges. These two parameters define the glass and brick surfaces, tilt angle, cavity depth, and orientation of the various surfaces. The cavity depth will be examined in three values: 0.3, 0.5, and 0.7 meters. For all modules except the vertical saw-tooth module, the ridge position in vertical distances of 1/3, 1/2, and 2/3 from the ridge to the module floor is considered. For the vertical saw-tooth module, these distances are horizontal from the ridge to the module edge with values of 1/3, 1/2, and 2/3. The number of modules on the classroom facade is 1×1, 2×2, or 4×4. The modules derived from these configurations create different WWRs. Structurally, the double-skin facade is of the box type with a 0.7-meter depth to analyze the research objective of the " double-skin self-shading facade" (Tables 4 and 5). The inner and outer skin details are described in Table 4.

### *4.2.3. Dependent variables of the research*

Energy performance in classroom heating, cooling, and lighting loads will be analyzed in all scenarios of vertical saw-tooth, horizontal saw-tooth, and triangular pyramid shapes throughout the year in kilowatt-hours.

Daylight metrics are divided into two parts: static and dynamic. The daylight calculation method can be categorized into static and dynamic or climate-based daylighting modeling (CBDM). DF as a static method can be introduced as the advanced attempt to measure daylighting[77]. Dynamic metrics, including SDA, UDI, ASE are proper for evaluating visual comfort and daylight-linked lighting controls [77,78]. The DF (static), which is static, is considered adequate for interior lighting according to CIBSE

**Table 5.** Double-layer self-shading façade settings (configurations) (cavity depth- ridge fold position - number of modules and different shapes).

| Sample plan double-skin self-shading | Sample plan flat double-skin | Basic sample plan |
|---|---|---|
| 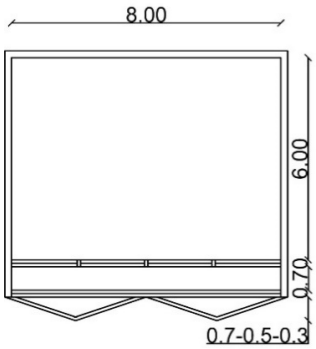  | 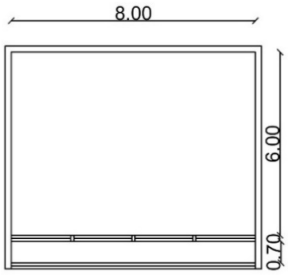  | 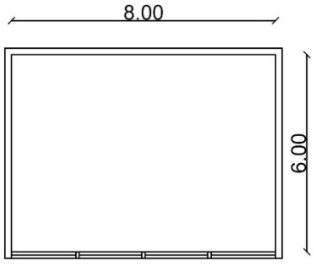  |
| Sample perspective double-skin self-shading | Sample perspective flat double-skin | Base sample perspective |
| 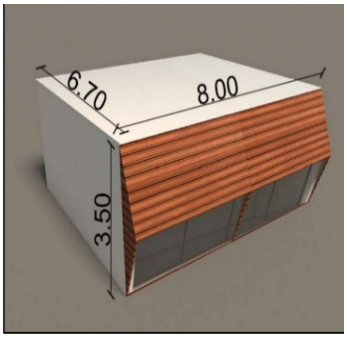  | 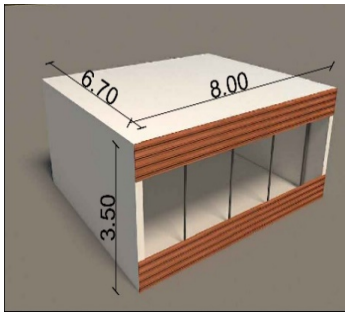  | 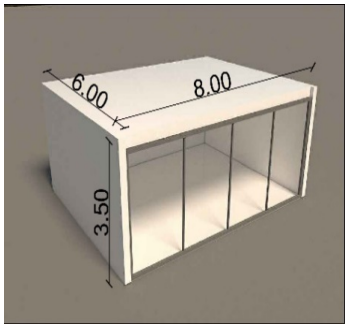  |
| | | Shape module double-skin self-shading |
| Triangular pyramid | Vertical saw-tooth | Horizontal saw-tooth |
| 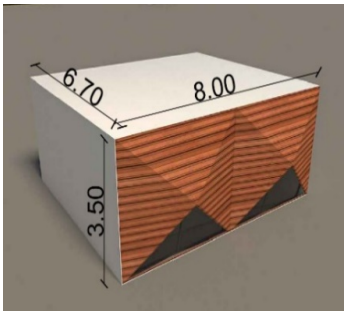  | 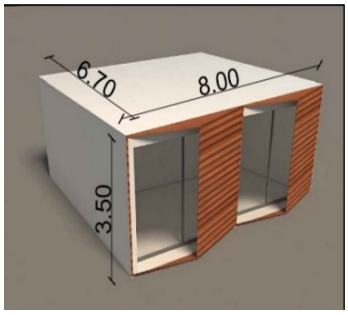  | 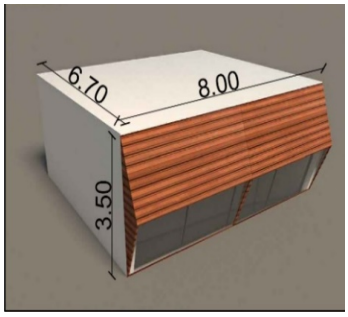  |

2383-8701/© 2024 The Author(s). Published by solarlits.com. This is an open access article under the CC BY license (https://creativecommons.org/licenses/by/4.0/).

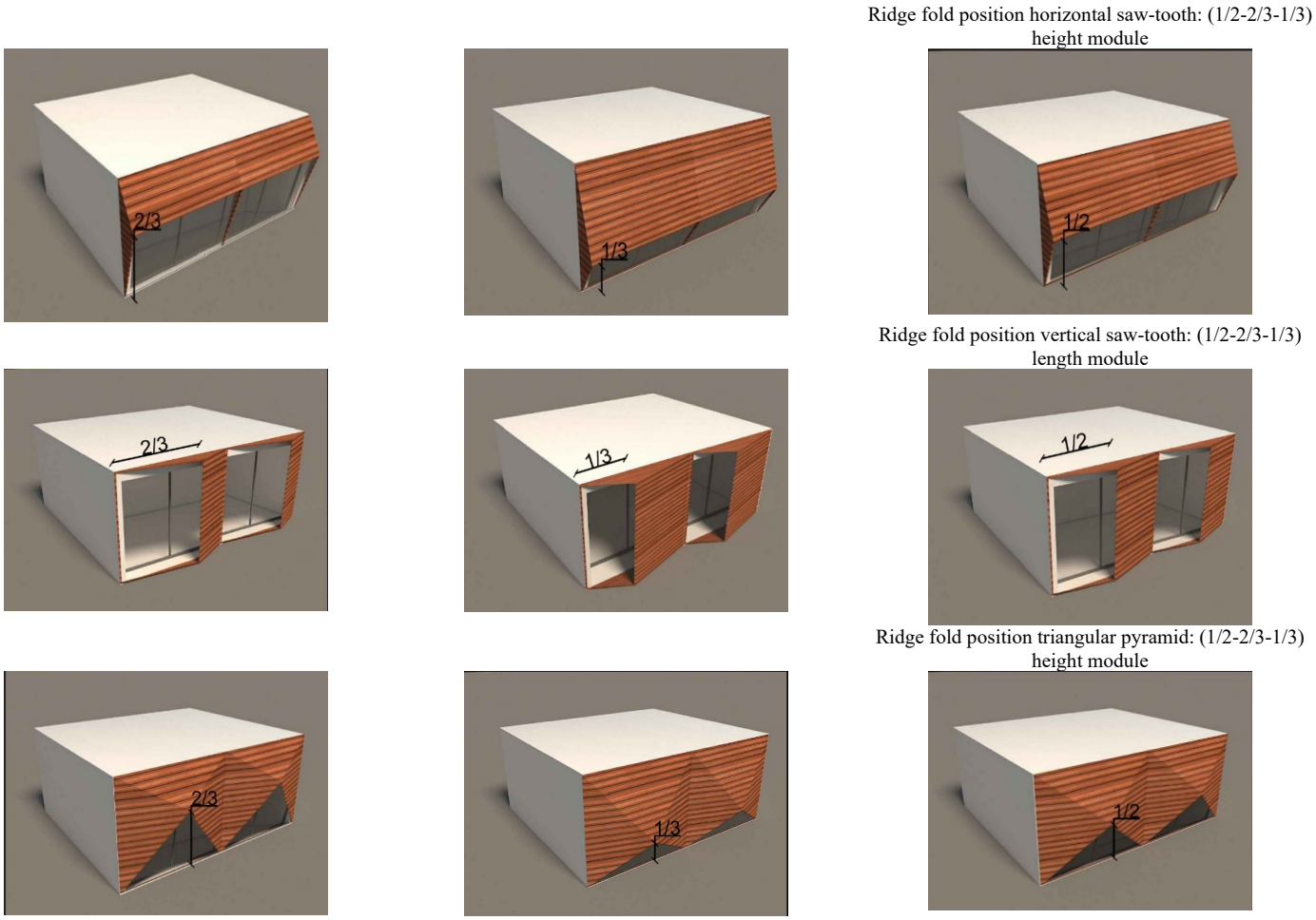


cavity depth triangular pyramid | Cavity depth vertical saw-tooth | Cavity depth horizontal saw-tooth

**Table 6.** The lowest heating, cooling, and lighting for vertical saw-tooth shape.

| Shape saw-tooth vertical | | | | |
|---|---|---|---|---|
| Load | Scenario | Number of modules | Ridge fold position | Cavity depth(m) |
| Cooling | 7 | 1×1 | 1/3 | 0.3 |
| Heating | 8 | 1×1 | 2/3 | 0.3 |

when it ranges between 2 and 5. Spaces may still need artificial lighting at times. Dynamic metrics include UDI, where the area without daylight has lighting below 150 lux for at least 50% of the occupied hours (UDI <150% 50%). The area with actual daylight is measured when daylight illuminance is in the 150-300 lux range for at least 50% of the occupied hours (UDI 150-300, ≥50%). The fully lit area with daylight includes only useful illuminance in the UDI 300-3000 range, 50% (UDI >3000 <5% + ≥50%). An area with illuminance above 3000 lux for at least 5% of the occupied hours (UDI >3000, ≥5%).For UDI, the passing threshold metric is defined as the percentage of occupied hours per year. So, a pass threshold value of 50% means that a given cell must achieve an illuminance of between 100 and 3000 lux (or whatever values were specified as the lux bounds in Calculation options) for at least 50% of the occupied hours in the year. SDA is measured as the percentage of occupied time throughout the year where the minimum illuminance threshold of 300 lux can be maintained with daylight alone. ASE is the number of hours in a year that a point on the work plane receives direct sunlight exceeding the usual threshold of 1000 lux. ASE is often used to quantify the risk of visual discomfort due to glare. The DGP scale is more intuitive and shows the percentage of people who feel uncomfortable in specific lighting conditions. A glare probability of 0.45 corresponds to unbearable glare, with an estimated 45% of people feeling discomfort under such lighting conditions, whereas a value of 0.35 is considered imperceptible.

## 5. Results

### *5.1. Energy performance*

The results show that comparing the flat facade with the double-skin self-shading facade, the heating load increased in most scenarios, but the cooling load decreased, and in all double-skin self-shading scenarios, lighting consumption significantly

2383-8701/© 2024 The Author(s). Published by solarlits.com. This is an open access article under the CC BY license (https://creativecommons.org/licenses/by/4.0/).

reduced. In most scenarios, the triangular pyramid, vertical saw-tooth, and horizontal saw-tooth shapes had the lowest cooling load. The lowest heating load was generated in most scenarios by the vertical saw-tooth, horizontal saw-tooth, and triangular pyramid shapes. The lowest heating, cooling, and lighting loads were for the three shapes: vertical saw-tooth (Table 6, Fig. 3), horizontal saw-tooth (Table 7, Fig. 4, triangular pyramid (Table 8, Fig. 5), and flat doble skin façade (Table 9, Fig. 6).

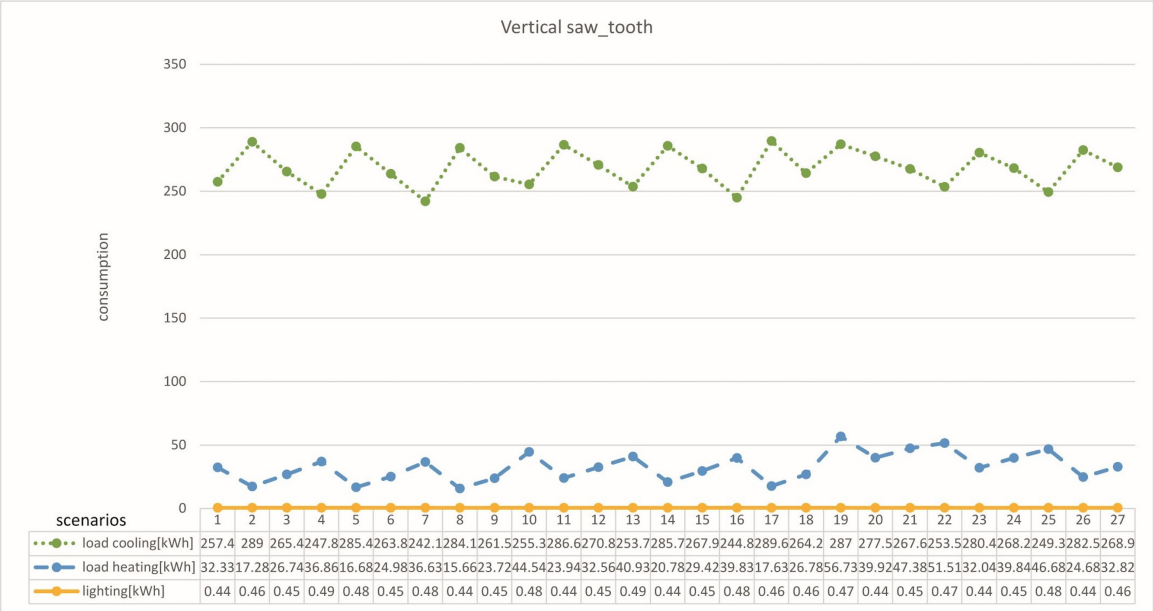


**Fig. 3.** Energy consumption of vertical saw-tooth shape.

**Table 7.** The lowest heating, cooling, and lighting for horizontal saw-tooth shape.

| Load | Scenario | Number of modules | Ridge fold position | Cavity depth(m) |
|---|---|---|---|---|
| Heating | 10 | 2×2 | 1/3 | 0.7 |
| Cooling | 16 | 2×2 | 1/3 | 0.3 |
| Lighting | 20 | 4×4 | 2/3 | 0.7 |

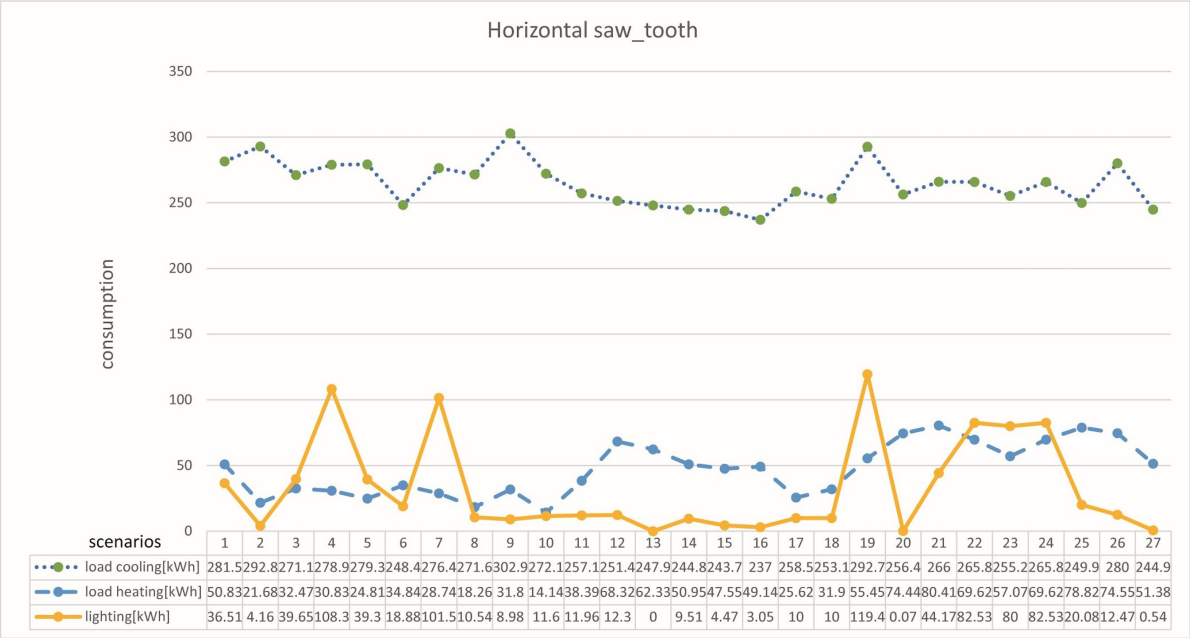


**Fig. 4.** Energy consumption of horizontal saw-tooth shape.

2383-8701/© 2024 The Author(s). Published by solarlits.com. This is an open access article under the CC BY license (https://creativecommons.org/licenses/by/4.0/).

### 5.2. Visual comfort

The DF of the double-skin flat facade is 8.8, indicating the potential for glare and excessive brightness, whereas, in most scenarios of the double-skin self-shading facade, sufficient lighting was between 2 and 5. The UDI daylight metrics: different shapes of the double-skin self-shading facade received over 70%, while the flat facade received 55%. SDA: The vertical saw-tooth shape provides the most SDA, followed by the horizontal saw-tooth and triangular pyramid shapes. The flat facade generates 100% SDA. ASE: In most scenarios, the vertical toothed module offers a more suitable ASE than the vertical saw-tooth and triangular pyramid shapes, with the flat facade showing a suitable 61%. DGP: Using the DAYSIM glare simulation software, all scenarios were re-modeled in Rhino software and graphically and quantitatively outputted using the Ladybug plugin to analyze glare in the classroom. All scenarios of the triangular pyramid and horizontal and vertical saw-tooth shapes had no glare problems. The daylight metrics for the scenarios of the vertical toothed (Fig. 7), horizontal saw-tooth (Fig. 8), triangular pyramid (Fig. 9), and flat facade (Fig. 10) were shown.

**Table 8.** The lowest heating, cooling, and lighting for triangular pyramid shape.

| load | scenario | Number of modules | ridge fold position | cavity depth(m) |
|---|---|---|---|---|
| heating | 11 | 2×2 | 2/3 | 0.7 |
| lighting | 26 | 4×4 | 2/3 | 0.3 |
| cooling | 27 | 4×4 | 1/2 | 0.3 |

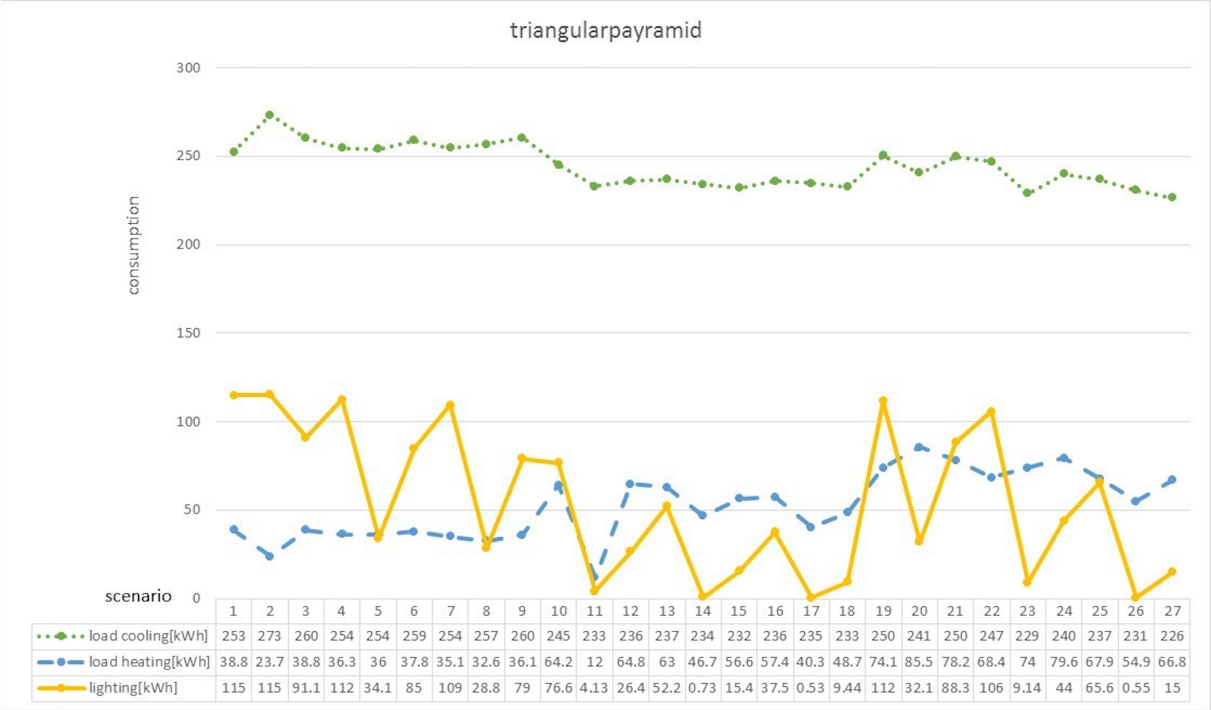


**Fig. 5.** Energy consumption of triangular pyramid shape.

**Table 9.** The lowest heating, cooling, and lighting for flat double-skin shape.

| Number of modules | Ridge fold position | Cavity depth(m) |
|---|---|---|
| 1×1 | 0 | 0.7 |

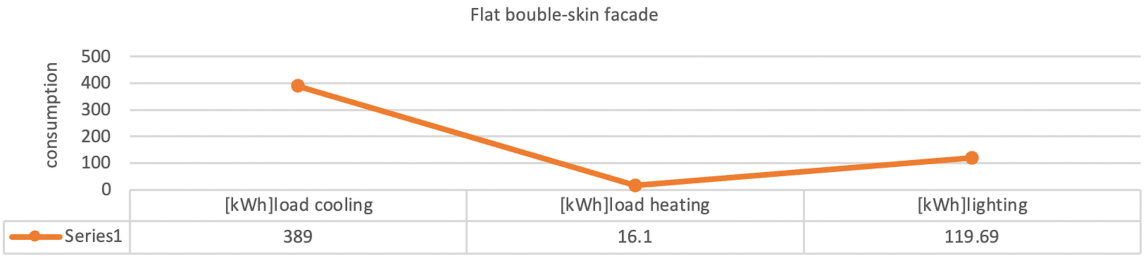


**Fig. 6.** Energy consumption of flat double-skin façade.

2383-8701/© 2024 The Author(s). Published by solarlits.com. This is an open access article under the CC BY license (https://creativecommons.org/licenses/by/4.0/).

### *5.3. Effect of double-skin self-shading facade parameters*

#### *5.3.1. Horizontal saw-tooth modul*

##### *5.3.1.1. Effect of ridge position fold with number of module (1×1)*

Results show that generally, the heating load increases for the ridge position fold 1/3 compared to the 1/2 and 2/3 positions. It is lower in the 2/3 ridge position fold, mainly due to a reduced glass surface area, reducing the potential for increased solar heat gain. The cooling load is low in these positions, and the cooling load trend is opposite to the heating load (the load increases with increasing ridge position fold). The shading impact in each module increases with the ridge position fold due to the increased tilt angle. However, this increase is influenced by the cavity depth discussed below. The lower ridge position allows a larger area for shading, resulting in significantly higher annual shading than other configurations. Lighting consumption at the 2/3 ridge position fold, with varying cavity depths, is lower than in other modules.

##### *5.3.1.2. Effect of cavity depth with number of module (1×1)*

Increasing cavity depth and various ridge positions fold to increase the heating load. Beyond a cavity depth of 0.7 meters, there is a sharp increase in heating load for the hypothesized closed-cavity design. This increase occurs, especially for the 1/3 folding position. Cooling load increases with a 0.3- meter cavity depth. Cavity depth affects heating and cooling loads due to changes in tilt angle and shading surface areas. The 0.7- meter cavity depth, influenced by ridge position fold compared to the 0.5 and 0.3- meter cavity depths, increases heating loads in various ridge positions fold. The 0.5- meter cavity depth reduces the cooling

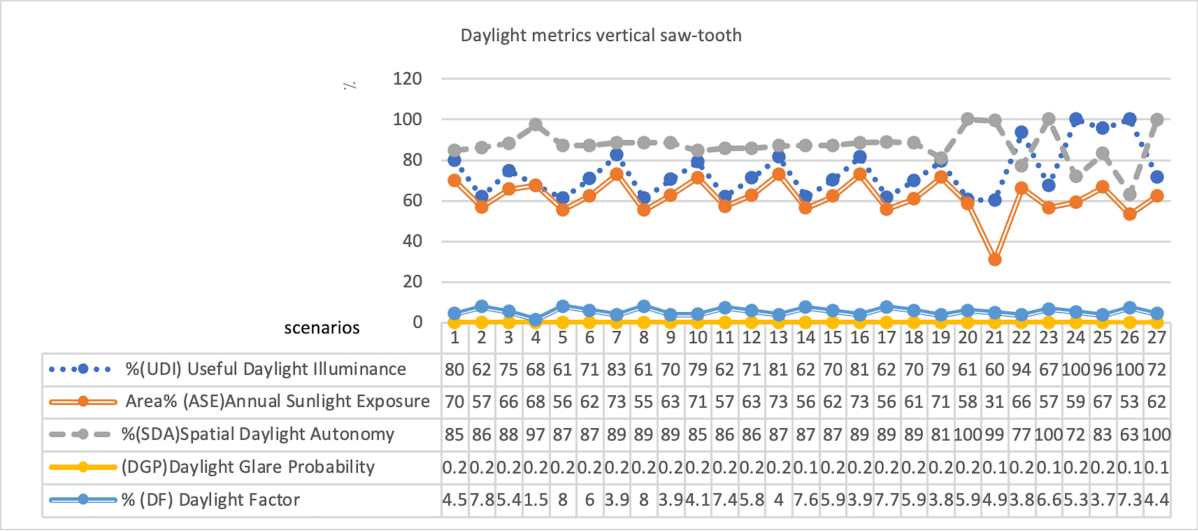


| scenarios | 1 | 2 | 3 | 4 | 5 | 6 | 7 | 8 | 9 | 10 | 11 | 12 | 13 | 14 | 15 | 16 | 17 | 18 | 19 | 20 | 21 | 22 | 23 | 24 | 25 | 26 | 27 |
|---|---|---|---|---|---|---|---|---|---|---|---|---|---|---|---|---|---|---|---|---|---|---|---|---|---|---|---|
| %(UDI) Useful Daylight Illuminance | 80 | 62 | 75 | 68 | 61 | 71 | 83 | 61 | 70 | 79 | 62 | 71 | 81 | 62 | 70 | 81 | 62 | 70 | 79 | 61 | 60 | 94 | 67 | 100 | 96 | 100 | 72 |
| Area% (ASE)Annual Sunlight Exposure | 70 | 57 | 66 | 68 | 56 | 62 | 73 | 55 | 63 | 71 | 57 | 63 | 73 | 56 | 62 | 73 | 56 | 61 | 71 | 58 | 31 | 66 | 57 | 59 | 67 | 53 | 62 |
| %(SDA)Spatial Daylight Autonomy | 85 | 86 | 88 | 97 | 87 | 87 | 89 | 89 | 89 | 85 | 86 | 86 | 87 | 87 | 87 | 89 | 89 | 89 | 81 | 100 | 99 | 77 | 100 | 72 | 83 | 63 | 100 |
| (DGP)Daylight Glare Probability | 0.2 | 0.2 | 0.2 | 0.2 | 0.2 | 0.2 | 0.2 | 0.2 | 0.2 | 0.2 | 0.2 | 0.2 | 0.2 | 0.1 | 0.2 | 0.2 | 0.2 | 0.2 | 0.2 | 0.2 | 0.1 | 0.2 | 0.1 | 0.2 | 0.2 | 0.1 | 0.1 |
| % (DF) Daylight Factor | 4.5 | 7.8 | 5.4 | 1.5 | 8 | 6 | 3.9 | 8 | 3.9 | 4.1 | 7.4 | 5.8 | 4 | 7.6 | 5.9 | 3.9 | 7.7 | 5.9 | 3.8 | 5.9 | 4.9 | 3.8 | 6.6 | 5.3 | 3.7 | 7.3 | 4.4 |

**Fig. 7.** Daylight metrics of vertical saw-tooth shape.

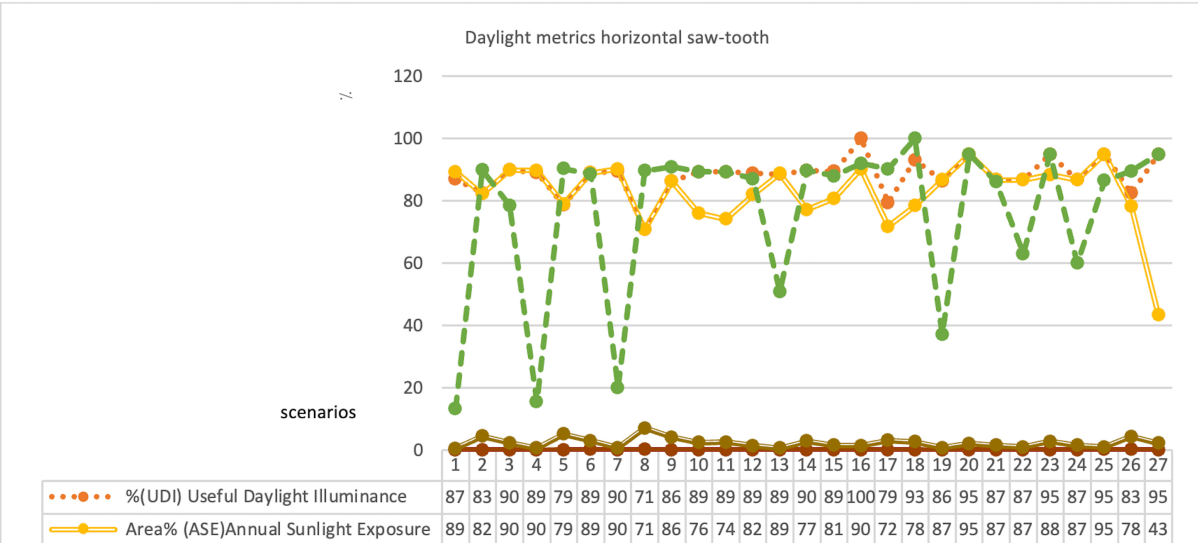


| scenarios | 1 | 2 | 3 | 4 | 5 | 6 | 7 | 8 | 9 | 10 | 11 | 12 | 13 | 14 | 15 | 16 | 17 | 18 | 19 | 20 | 21 | 22 | 23 | 24 | 25 | 26 | 27 |
|---|---|---|---|---|---|---|---|---|---|---|---|---|---|---|---|---|---|---|---|---|---|---|---|---|---|---|---|
| %(UDI) Useful Daylight Illuminance | 87 | 83 | 90 | 89 | 79 | 89 | 90 | 71 | 86 | 89 | 89 | 89 | 89 | 90 | 89 | 100 | 79 | 93 | 86 | 95 | 87 | 87 | 95 | 87 | 95 | 83 | 95 |
| Area% (ASE)Annual Sunlight Exposure | 89 | 82 | 90 | 90 | 79 | 89 | 90 | 71 | 86 | 76 | 74 | 82 | 89 | 77 | 81 | 90 | 72 | 78 | 87 | 95 | 87 | 87 | 88 | 87 | 95 | 78 | 43 |
| %(SDA)Spatial Daylight Autonomy | 13 | 90 | 79 | 15 | 90 | 89 | 20 | 90 | 91 | 89 | 89 | 87 | 51 | 90 | 88 | 92 | 90 | 100 | 37 | 95 | 86 | 63 | 95 | 60 | 87 | 90 | 95 |
| (DGP) Daylight Glare Probability | 0.2 | 0.2 | 0.2 | 0.1 | 0.2 | 0.2 | 0.2 | 0.2 | 0.2 | 0.1 | 0.2 | 0.1 | 0.1 | 0.2 | 0.1 | 0.1 | 0.2 | 0.1 | 0.1 | 0.2 | 0.1 | 0.1 | 0.2 | 0.1 | 0.2 | 0.2 | 0.2 |
| % (DF) Daylight Factor | 0.6 | 4.5 | 2.4 | 0.7 | 5.2 | 3.1 | 0.8 | 7.1 | 4.2 | 2.5 | 2.5 | 1.4 | 0.7 | 2.9 | 1.6 | 1.5 | 3.2 | 2.7 | 0.8 | 2.2 | 1.6 | 1.1 | 2.8 | 1.6 | 1 | 4.4 | 2.2 |

**Fig. 8.** Daylight metrics of horizontal saw-tooth shape.

2383-8701/© 2024 The Author(s). Published by solarlits.com. This is an open access article under the CC BY license (https://creativecommons.org/licenses/by/4.0/).

load, and the 0.3- meter cavity depth reduces the heating load and increases the cooling load. This is partly due to the lower shading impact in winter and summer from the upper fold and a reduced tilt angle. With increased shading area, lighting consumption generally increases with a larger cavity. Lighting consumption for modules with a 0.7- meter cavity is less than in other modules.

#### *5.3.1.3. Effect of the number of modules*

Increasing the number of folds increases the shading surface area. Increasing the number of modules increases the heating load due to increased surface area, reduced slope, and shading by adjacent units. The 1×1 module has the lowest heating load. The 2×2 module has the lowest cooling load and moderate heating load.

Finally, the best horizontal saw-tooth module for heating load is a 0.7-meter cavity depth, a 1/3 ridge position fold, and a 2×2 module configuration. It has a 0.3-meter cavity depth, a 1.3 ridge position, and a 2×2 module configuration for cooling load. Lighting consumption is lowest for the 0.7-meter cavity depth, 2/3 ridge position fold, and 4×4 module configuration (Table 10).

### *5.3.2. Vertical saw-tooth module*

#### *5.3.2.1. Effect of ridge position fold with number of module (1×1)*

These scenarios are similar to the horizontal saw-tooth module heating load increases for the 1/3 ridge position fold due to the reduced glass surface area. Cooling load behaves inversely, increasing with a higher ridge position fold.

#### *5.3.2.2. Effect of cavity depth with number of module (1×1)*

Increasing cavity depth raises the heating and cooling loads. Reduced cavity depth decreases the heating and cooling loads. Cavity depth affects shading angle changes.

#### *5.3.2.3. Effect of the Number of Modules*

Examining different depths and ridge positions fold, increasing the folds enhances the shading surface area while increasing heating and cooling loads. The 1×1 number of module configurations has more optimal heating and cooling loads. Ultimately, the best vertical saw-tooth module for heating load has the 2/3 ridge

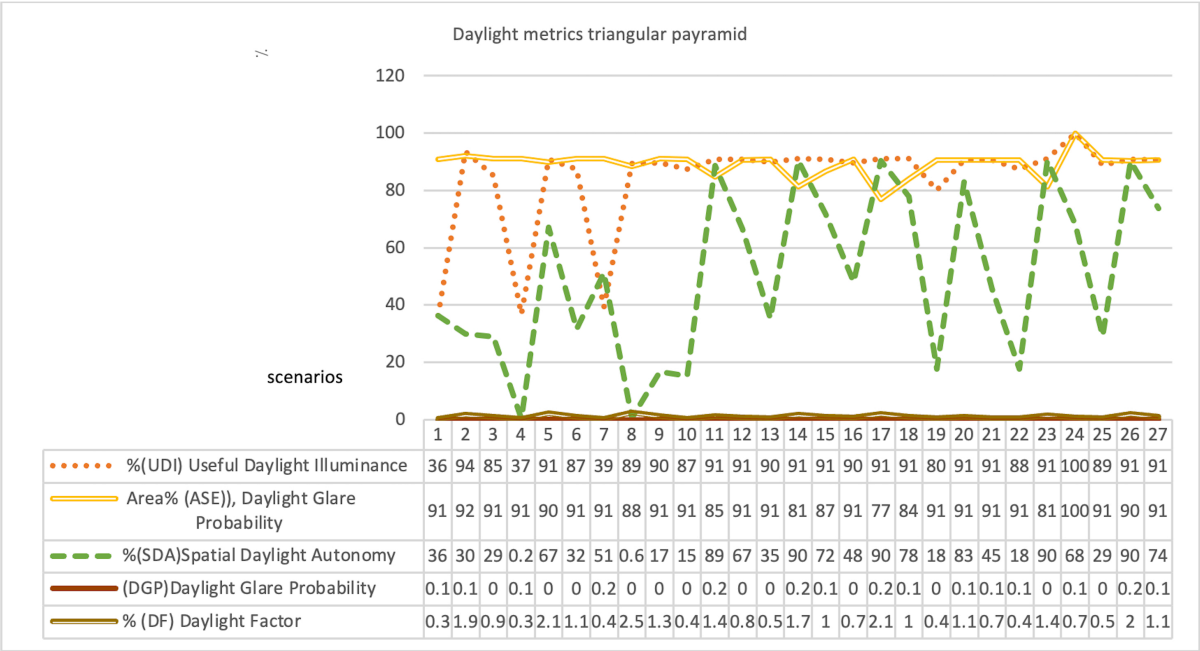


| scenarios | 1 | 2 | 3 | 4 | 5 | 6 | 7 | 8 | 9 | 10 | 11 | 12 | 13 | 14 | 15 | 16 | 17 | 18 | 19 | 20 | 21 | 22 | 23 | 24 | 25 | 26 | 27 |
|---|---|---|---|---|---|---|---|---|---|---|---|---|---|---|---|---|---|---|---|---|---|---|---|---|---|---|---|
| %(UDI) Useful Daylight Illuminance | 36 | 94 | 85 | 37 | 91 | 87 | 39 | 89 | 90 | 87 | 91 | 91 | 90 | 91 | 91 | 90 | 91 | 91 | 80 | 91 | 91 | 88 | 91 | 100 | 89 | 91 | 91 |
| Area% (ASE)), Daylight Glare Probability | 91 | 92 | 91 | 91 | 90 | 91 | 91 | 88 | 91 | 91 | 85 | 91 | 91 | 81 | 87 | 91 | 77 | 84 | 91 | 91 | 91 | 91 | 81 | 100 | 91 | 90 | 91 |
| %(SDA)Spatial Daylight Autonomy | 36 | 30 | 29 | 0.2 | 67 | 32 | 51 | 0.6 | 17 | 15 | 89 | 67 | 35 | 90 | 72 | 48 | 90 | 78 | 18 | 83 | 45 | 18 | 90 | 68 | 29 | 90 | 74 |
| (DGP)Daylight Glare Probability | 0.1 | 0.1 | 0 | 0.1 | 0 | 0 | 0.2 | 0 | 0 | 0 | 0.2 | 0 | 0 | 0.2 | 0.1 | 0 | 0.2 | 0.1 | 0 | 0.1 | 0.1 | 0.1 | 0 | 0.1 | 0 | 0.2 | 0.1 |
| % (DF) Daylight Factor | 0.3 | 1.9 | 0.9 | 0.3 | 2.1 | 1.1 | 0.4 | 2.5 | 1.3 | 0.4 | 1.4 | 0.8 | 0.5 | 1.7 | 1 | 0.7 | 2.1 | 1 | 0.4 | 1.1 | 0.7 | 0.4 | 1.4 | 0.7 | 0.5 | 2 | 1.1 |

**Fig. 9.** Daylight metrics of triangular payramid shape.

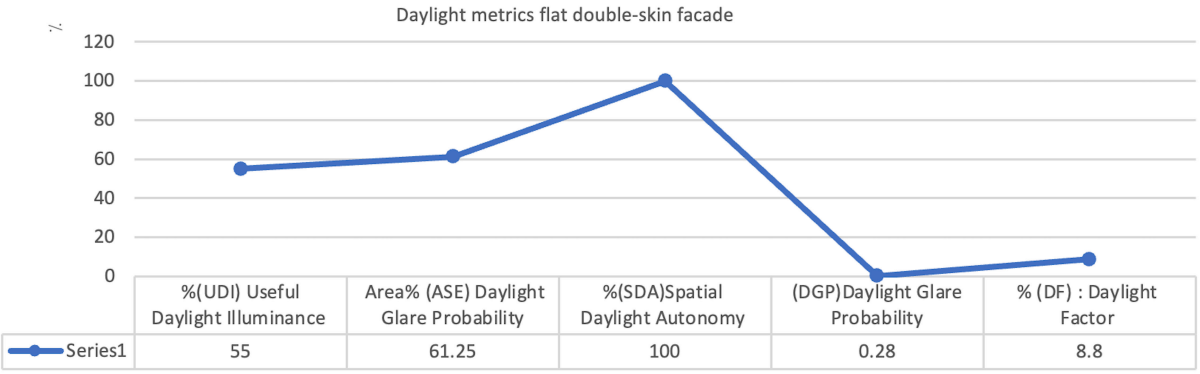


| | %(UDI) Useful Daylight Illuminance | Area% (ASE) Daylight Glare Probability | %(SDA)Spatial Daylight Autonomy | (DGP)Daylight Glare Probability | % (DF) : Daylight Factor |
|---|---|---|---|---|---|
| Series1 | 55 | 61.25 | 100 | 0.28 | 8.8 |

**Fig. 10.** Daylight metrics of flat double-skin façade.

2383-8701/© 2024 The Author(s). Published by solarlits.com. This is an open access article under the CC BY license (https://creativecommons.org/licenses/by/4.0/).

position fold, a 0.3-meter cavity depth, and a 1×1 number of module configurations. The best cooling load is the 1/3 ridge position fold, a 0.3-meter cavity depth, and a 1×1 number of module configurations. Lighting consumption remains relatively constant across the modules (Table 10).

### *5.3.3. Triangular pyramid module*

#### *5.3.3.1. Effect of ridge position folds with number of module (1×1)*

The impact of the ridge position fold on heating and cooling loads follows a similar trend observed in the horizontal saw-tooth scenarios. The heating load is higher at the 1/3 ridge position fold due to reduced glass surface area and increased shading, which decreases passive heat inside the space. Heating load is lowest at the 2/3 ridge position fold. The 2/3 ridge position fold increases the cooling load due to more passive heat and reduced shading, which is lowest at the 1/3 ridge position fold. Lighting consumption is lowest at the 2/3 ridge position fold.

#### *5.3.3.2. Effect of cavity depth with number of module (1×1)*

Increasing cavity depth reduces the heating load in different ridge positions fold. Conversely, the cooling load decreases with more considerable cavity depths. A 0.5-meter cavity depth reduces the cooling load and increases the heating load. Cavity depth also affects shading due to related changes in orientation and tilt angle. Lighting consumption is lowest for a 0.3-meter cavity depth.

#### *5.3.3.3. Effect of the number of modules*

Increasing the number of folded units in the studied facade module increases the heating load and reduces the cooling load. This increase is particularly pronounced with greater cavity depth. The increase in cooling load is less significant with smaller cavity depths. The shading surface area significantly increases with more modules. The best triangular pyramid module for heating load is at the 2/3 ridge position fold, with a 0.7-meter cavity depth and a 2×2 number of module configuration. For cooling load, it is at the 1/2 ridge position fold, with a 0.3-meter cavity depth and a 4×4 number of module configuration. Lighting consumption is lowest for the 2/3 ridge position fold, with a 4×4 number of module configuration and a 0.3-meter cavity depth (Table 10).

## 6. Discussion

After examining the annual energy performance of the double-skin flat facade, the cooling load increases due to the greenhouse effect, which is consistent with previous research. Adding the self-shading facade strategy through the three sloped forms, horizontal saw-tooth, vertical saw-tooth, and triangular pyramid, to the box-type double-skin structure reduces cooling load by controlling direct sunlight and light penetration into the space. This aligns with previous research [56,58], which introduced conventional shading devices to reduce cooling load. The brick material of the self-shading facade also positively affects the double-skin cavity due to its high thermal mass, reducing the cavity air temperature during summer, thus significantly decreasing the cooling load

**Table 10.** The top three scenarios of the double-skin self-shading façade.

| | Double-skin self-shading facade | Specifications | |
|---|---|---|---|
| 1 | 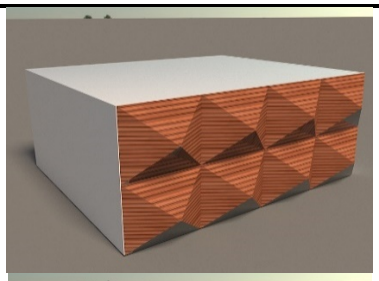 | Shape module :triangular payramid<br>ridge position fold:2/3 height module<br>cavity depth: 0.7m<br>number of module: 2×2 | Load cooling: 232 KWH<br>Load heating: 12KWH<br>lighting: 4 KWH<br>UDI :90%<br>ASE : 84%<br>SDA :88%<br>DGP :0.16<br>DF: 1.37 |
| 2 | 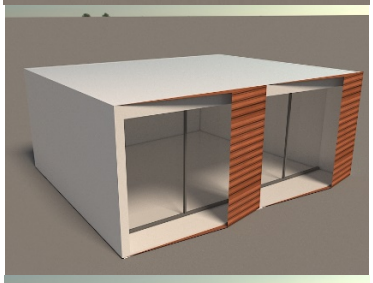 | Shape module : vertical saw-tooth<br>ridge position fold:2/3 height module<br>cavity depth: 0.3m<br>number of module: 1×1 | Load cooling: 284 KWH<br>Load heating: 15KWH<br>lighting: 0.44 KWH<br>UDI :61%<br>ASE : 55%<br>SDA :88%<br>DGP :0.2<br>DF: 8 |
| 3 | 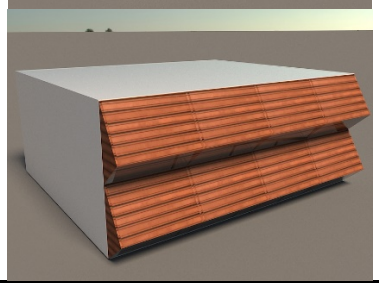 | Shape module : Horizontal saw-tooth<br>ridge position fold:1/3 height module<br>cavity depth: 0.7m<br>number of module: 2×2 | Load cooling: 272 KWH<br>Load heating: 14KWH<br>lighting: 11 KWH<br>UDI: 89%<br>ASE : 76%<br>SDA: 89%<br>DGP: 0.1<br>DF :2.5 |

2383-8701/© 2024 The Author(s). Published by solarlits.com. This is an open access article under the CC BY license (https://creativecommons.org/licenses/by/4.0/).

[59]. The best scenario for reducing the cooling load is the triangular pyramid module with a 1/2 ridge position fold, 4×4 number of module configuration, 0.3- meter cavity depth, and 226 kWh energy consumption.

The heating load in most double-skin self-shading facade scenarios is higher than in the double-skin flat facade. This effect is due to the sloped walls [35,36]. However, some shapes in this strategy show a lower heating load than the double-skin flat facade. The cavity depth of the double-skin self-shading facade reduces the thermal conductivity of external surfaces and preheats the interior space. Smaller cavity depths create a more pronounced chimney effect, moving warm air [66]. Also, using single-pane glass in the first layer and double-skin glass in the second layer enhances this effect in the double-skin scenarios [67,68]. The best scenario for reducing heating load, even less than the double-skin flat facade, is the triangular pyramid shape with a 2/3 ridge position fold, a 2×2 number of module configuration, a 0.7-meter cavity depth, and 12 kWh energy consumption.

Lighting consumption is lower in the three self-shading facade shapes than in the double-skin flat facade, with the vertical saw-tooth shape scenarios having the lowest average of 0.45 kWh. This is due to the vertical glass forms and better daylight reception than the other two shapes. The double-skin self-shading facade, by tilting the walls and using modular fixed shading, scatters direct sunlight and improves indoor light quality, consistent with previous studies [24-32,33]. Furthermore, the sloped walls in this strategy play a crucial role in controlling sunlight in the interior space [48] and are vital in determining DA levels and reducing glare [47].

The best scenario for achieving the average daylight factor (DF) is the vertical saw-tooth shape due to the glass forms exceeding 2%. The highest beneficial daylight illuminance (UDI), thanks to

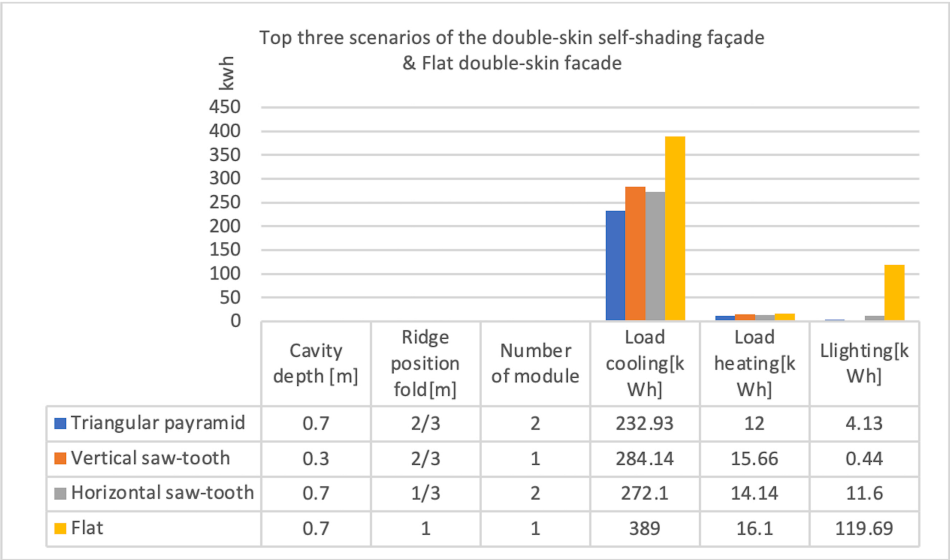


| | Cavity depth [m] | Ridge position fold[m] | Number of module | Load cooling[kWh] | Load heating[kWh] | Llighting[kWh] |
|---|---|---|---|---|---|---|
| Triangular payramid | 0.7 | 2/3 | 2 | 232.93 | 12 | 4.13 |
| Vertical saw-tooth | 0.3 | 2/3 | 1 | 284.14 | 15.66 | 0.44 |
| Horizontal saw-tooth | 0.7 | 1/3 | 2 | 272.1 | 14.14 | 11.6 |
| Flat | 0.7 | 1 | 1 | 389 | 16.1 | 119.69 |

**Fig. 11.** Comparison energy consumption between flat double-skin façade and top three scenarios of the double-skin self-shading façade.

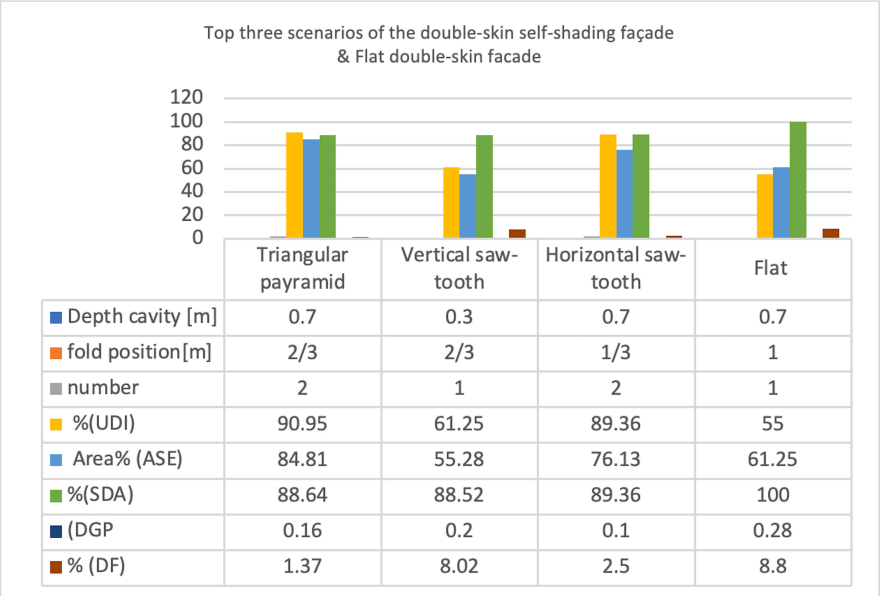


| | Triangular payramid | Vertical saw-tooth | Horizontal saw-tooth | Flat |
|---|---|---|---|---|
| Depth cavity [m] | 0.7 | 0.3 | 0.7 | 0.7 |
| fold position[m] | 2/3 | 2/3 | 1/3 | 1 |
| number | 2 | 1 | 2 | 1 |
| %(UDI) | 90.95 | 61.25 | 89.36 | 55 |
| Area% (ASE) | 84.81 | 55.28 | 76.13 | 61.25 |
| %(SDA) | 88.64 | 88.52 | 89.36 | 100 |
| (DGP | 0.16 | 0.2 | 0.1 | 0.28 |
| % (DF) | 1.37 | 8.02 | 2.5 | 8.8 |

**Fig. 12.** Comparison daylight metrics between flat double-skin façade and top three scenarios of the double-skin self-shading façade.

2383-8701/© 2024 The Author(s). Published by solarlits.com. This is an open access article under the CC BY license (https://creativecommons.org/licenses/by/4.0/).

the glass extending close to the classroom floor, are the horizontal saw-tooth, triangular pyramid, and vertical saw-tooth scenarios, respectively, while the flat double-skin facade achieves 55%. Daylight autonomy (SDA) and annual sunlight exposure (ASE) are suitable and better in the vertical saw-tooth shape than in the other two. The flat double-skin facade provides 100% SDA and 60% suitable ASE. Analyzing the daylight glare probability (DGP) criterion, all double-skin self-shading scenarios perform better in glare-free spaces due to the tilted form than the double-skin flat facade. Figures 11 and 12 show a comparison between double-skin self-shading facade and the double-skin flat facade.

## 7. Conclusion

To present a new solution for designing high-performance school building facades that control direct sunlight and daylight penetration to improve energy consumption and visual comfort, this article proposes a modular brick double-skin self-shading facade for traditional, flat double-skin facades. The components and settings of the double-skin self-shading, flat double-skin, and base model scenarios were presented.

A comparison of the results between the double-skin self-shading and flat double-skin facades reveals the following:

1. Overall, the double-skin self-shading facade, with its horizontal saw-tooth, vertical saw-tooth, and triangular pyramid forms, reduced the cooling load from 389 kWh (flat double-skin) to an average of 260 kWh. The triangular pyramid scenarios had the most significant cooling load reduction, indicating the positive effect of external shading on double-skin performance.
2. Despite reducing the cooling load, the double-skin self-shading facade increased the heating load in most configurations of the three forms, except in three scenarios with a lower heating load than the flat double-skin facade. This increase in heating load is due to the sloped and double-skin nature of the self-shading facade.
3. The double-skin self-shading facade increases daylight in the classroom compared to the flat double-skin facade. This solution allows students to use the areas near windows better by reducing the thermal conductivity of external surfaces and preheating the interior space. Consequently, reduced lighting consumption is evident across all double-skin self-shading scenarios. This reduction is also due to the sloped structure and glass extending to the classroom floor.
4. Regarding glare in the classroom, the double-skin self-shading facade scenarios produced an acceptable and suitable DGP level, performing even better than the flat double-skin facade.
5. The box structure of the double-skin self-shading facade reduces noise in the classroom environment and minimizes fire hazards.

Using similar solutions as this research can significantly impact designers' workflows, resident comfort, and environmental conservation. With its cavity and double-skin facade potential, the double-skin self-shading facade can efficiently address classroom ventilation and student thermal comfort, which can be further explored in future research. The proposed solution can also be adapted with photovoltaic panels and energy generation for warm and cold climates globally, not just Isfahan's hot and dry climate.

## Acknowledgement

This research received no specific grant form any funding agency in the public, commercial, or not-for-profit sectors.

## Contributions

S. Aghamohammadiha: Conceptualization, Methodology, Simulation, Writing the initial draft, Writing- Original draft preparation, investigation and data analysis, Visualization, Writing-review & editing. N. Dehghan: Conceptualization, Methodology, Supervision and Reviewing.

## Declaration of competing interest

The authors declare no conflict of interest.

## References

[1] I. Farrou, M. Kolokotroni, M. Santamouris, Building envelope design for climate change mitigation:a case study of hotels in Greece, Sustainable Energy, 35 (2016) 944-967.
[2] D., Rutz, Transition towards a sustainable heating and cooling sector-case study of southeast European countries, Thermal Science, 23 (2019) 269-269.
[3] A. Thewes, S. Maas, F. Scholzen , D. Waldmann, A. Zürbes, Field study on the energy consumption of school buildings in Luxembourg, Energy and Buildings, 68 (2014) 460-470.
[4] Iranian Fuel Conservation Organization, Modification of Energy Consumption Patterns in Schools and Offices, Iran Ministry of Energy: Tehran, 2009, pp. 18-30.
[5] P. Im , J. Haberl, A survey of high performance schools, in: Proceedings of the Fifteenth Symposium on Improving Building Systems in Hot and Humid Climates, Orlando, FL, (24-26 July 2006), pp. 1-10.
[6] M. Liu , K. Wittchen , P. Heiselberg, Control strategies for intelligent glazed façade and their influence on energy and comfort performance of office buildings in Denmark, Applied Energy, 145 (2015) 43-51.
[7] M. M. Shahda, Self-Shading Walls to Improve Environmental Performance in Desert Buildings, academia.edu, 10 (1) (2020) 1-14.
[8] I. Guedi Capeluto, Energy performance of the self-shading building envelope, Energy and Buildings, 35 (2003) 327-336.
[9] S. Giostra, L. Blough, Folded-BISC:a parametric design approach to building integrated solar collectors, in:11th Conference on Advanced Building Skins, Bern, Switzerland, (10-11 oct 2016), pp. 1-19.
[10] N. Djongyang, Thermal comfort: a review paper, Renewable, and Sustainable Energy Reviews, 14 (2010) 2626-2640.
[11] J. van Hoof, Forty years of Fanger's model of thermal comfort: comfort for all?, Indoor Air, 18(3) (2003) 182-201.
[12] R. J. de Dear, Progress in thermal comfort research over the last twenty years, Indoor Air, 23(6) (2013) 442-461.
[13] E. Oesterle, Double-skin Facades - Integrated Planning , Prestel Verlag: Munich, Germany, 2001, pp. 1-252.
[14] M., Joshghani, Cooling and heating energy consumption in school buildings, New School, 26 (2001)18-20.
[15] S. C. Zerefos, C. A. Tessas, A. M. Kotsiopoulos, D. Founda, A. Kokkini, The role of building form in energy consumption: The case of a prismatic building in Athens, Energy and Buildings, 48 (2012) 97-102.
[16] S. S. Saifelnasr, Design of a Self-Shading Mass as a Function of the Latitude for Automatic Seasonal Adjustment, in: IOP Conference Series: Earth and Environmental Science, Cardiff, Wales, (24-25 September 2019), pp. 1-8.
[17] M. Nikpour, M. z. Kandar, M. Ghasemi, M. Ghomeshi, M. r. Safizadeh, Heat Transfer Reduction Using Slef Shading Strategy in Energy Commission Building in Malasiya, journal of applied sciences, 12(9) (2012) 897-901.
[18] Y. Lavafpour, S. Sharples, Summer Thermal Comfort and Self-Shading Geometries in Passivhaus Dwellings: A Pilot Study Using Future UK Climates, buildings, 5(3) (2015) 964-984.
[19] A. L. S. Chan, T. T. Chow, Thermal performance of air-conditioned office buildings constructed with inclined walls in different climates in China, Applied Energy, 114 (2014) 45-57.
[20] M. Z. Kandar, P. S. Nimlyat, M. G. Abdullahi, Y. A. Dodo, Influence of inclined wall self-shading strategy on office building heat gain and energy performance in hot humid climate of Malaysia, Heliyon, 5 (2019) 1-10.

2383-8701/© 2024 The Author(s). Published by solarlits.com. This is an open access article under the CC BY license (https://creativecommons.org/licenses/by/4.0/).

[21] W.S.S.W.M. Rashdi, M.R. Embi, Analysing Optimum Building Form in Relation to Lower Cooling Load, Procedia-Social and Behavioral Sciences, 222 (2016) 782-790.
[22] K. Tarabieh, S. Abdelmohsen, A. Hassan, R. El-Dabaa, Y. Elghazi, Parametric Investigation of Brick Extrusion Patterns Using Thermal Simulation, in: 4th Building Simulation and Optimization Conference, Cambridge, UK., (11-12 September 2018), pp. 597-604.
[23] M. Latifi Khorasani, J. Burry, M. Salehi, Thermal performance of patterned facades, eCAADe, 1 (2015) 267-276.
[24] A., Aksamija, Sustainable Facades: Design Methods for High-Performance Building Envelopes, Wiley: Germany, 2013, pp. 1-240.
[25] S. d. Rahimzadeh, V. Garcia Hansen, R. Drogemuller, G. Isoardi, Parametric Modelling for the Efficient Design of Daylight Strategies with ComPlex Geometries, in: 47th International Conference of the Architectural Science Association, Australia, (2013), pp. 449-458.
[26] M. L. Beaman, S. Bader, Responsive Shading Intelligent Façade Systems, ACADIA, 13 (2010) 263-269.
[27] N. Emami, A. Khodadadi, P. V. Buelow, Design of Shading Screen Inspired by Persian Geometric Patterns: An Integrated Structural and Daylighting Performance Evaluation, in: Shells, Membranes and Spatial Structures, Brasilia, Brazil, (2014), pp. 1-8.
[28] H. Kim, M. J. Clayton, A multi-objective optimization approach for climate-adaptive building envelope design using parametric behavior maps, Building and Environment, 185 (2020) 107292.
[29] H. Kim, M. J. Clayton, Parametric behavior maps: A method for evaluating the energy performance of climate-adaptive building envelopes, Energy & Buildings, 219(2) (2020) 110020.
[30] S. M. Hosseini, M. Mohammadi, O. Guerra-Santin, Interactive kinetic façade: Improving visual comfort based on dynamic daylight and occupant's positions by 2D and 3D shape changes, Building and Environment, 165 (2019) 106396.
[31] A. H. Ahmed Mahmoud, Y. Elghazi, Parametric-based designs for kinetic facades to optimize daylight performance: Comparing rotation and translation kinetic motion for hexagonal facade patterns, Solar Energy, 126 (2016)111-127.
[32] A. Narangerel, J.-H. Lee, R. Stouffs, Daylighting Based Parametric Design Exploration of 3D Facade Patterns, eCAADe, 2 (2016) 379-388.
[33] A. Narangerel, J.-H. Lee, R. Stouffs, Thermal and Daylighting Optimization of Complex 3D Faceted Façade for Office Building, eCAADe, 2 (2017) 183-192.
[34] A. Vergauwen, L. Alegria Mira, K. Roovers, N. De Temmerman, Parametric design of adaptive shading elements based on Curved-line Folding, in: Proceedings of the First Conference Transformables, Spain, (2013), pp. 1-6.
[35] C. Hachem, M. Elsayed, Patterns of façade system design for enhanced energy performance of multistory buildings, Energy & Building, 130 (2016) 366-377.
[36] C. Hachem-Vermette, Multistory building envelope: Creative design and enhanced performance, Solar Energy, 159 (2018) 710-721.
[37] E., Kızılörenli, A. Tokuç, Parametric Optimization of a Responsive Façade System for Daylight Performance, Journal of Architectural Sciences and Applications, 7(1) (2022) 72-81.
[38] K. Lakhdari, L. Sriti, B. Painter, Parametric optimization of daylight, thermal and energy performance of middle school classrooms, case of hot and dry regions, Building and Environment, 204(2) (2021) 08173.
[39] K. S. Galal, The impact of classroom orientation on daylight and heat-gain performance in the Lebanese Coastal zone, Alexandria Engineering Journal, 58(3) (2019) 827-839.
[40] H. Aibaghi Esfahani, K. Momeni, F. Hasanpor, Impact of Building Orientation on Annual Energy Consumption in Schools in Hot Arid Regions in Iran, Using Climate Modeling, Case Study: A Double-class School, Armanshahr Architecture & Urban Development, 14(34) (2021) 23-40.
[41] A. A.Y. Freewan, Advances in Passive Cooling Design: An Integrated Design Approach, IntechOpen: Rijeka, 2019, pp. 1-158.
[42] S. C. Anna Pellegrinoa, Valeria Savio, Daylighting for Green schools: a resource for indoor quality and energy efficiency in educational environments, Energy Procedia, 78 (2015) 3162-3167.
[43] J. A. A. D. Ahmed A.Y. Freewan, Assessment of daylight performance of Advanced Daylighting Strategies in Large University Classrooms; Case Study Classrooms at JUST, Alexandria Engineering Journal, 59 (2019) 791-802.
[44] C. Y. L. María Beatriz Piderit Moreno Methodology for Assessing Daylighting Design Strategies in Classroom with a Climate-Based Method, Sustainability, 7 (2015) 880-897.
[45] L. P. L Callejas, A Reyes, P Torres, B Piderit, Optimization of Natural Lighting Design for Visual Comfort in Modular Classrooms: Temuco Case, in: IOP Conference Series: Earth and Environmental Science, Temuco, Chile (16-18 October 2019), pp. 1-13.
[46] Y. Y. Yang Guan Daylighting Design in Classroom Based on Yearly-Graphic Analysis, sustainability, 8 (2016) 604 610.
[47] P. Bakmohammadi, E. Noorzai, Optimization of the design of the primary school classrooms in terms of energy and daylight performance considering occupants' thermal and visual comfort, Energy Reports, 6 (2020) 1590-1607.
[48] Atthaillah, R. A. Mangkuto, M. D. Koerniawan, J. L. M. Hensen, B. Yuliarto, Optimization of Daylighting Design Using Self-Shading Mechanism in Tropical School Classrooms with Bilateral Openings, Journal of Daylighting, 9(2) (2022) 117-136.
[49] V., Zepatou, School Facilities and Sustainability-Related Concepts: A Study of Hellenic Secondary School Principals', Teachers', Pupils' and Parents' Responses. Sustainability, 8(4) (2016) 311-339.
[50] A. Kirimtat, Koyunbaba, B.K., Chatzikonstantinou, I., Sariyildiz, S, Review of simulation modeling for shading devices in buildings, Renewable and Sustainable Energy Reviews, 53 (2016) 23-49.
[51] N. A. Al-Tamimi, Fadzil, S.F.S, The potential of shading devices for temperature reduction in high-rise residential buildings in the tropics., Procedia Engineering, 21 (2011) 273-282.
[52] T. E. Kuhn, Bühler, C., Platzer, W.J, Evaluation of overheating protection with sunshading systems, Solar Energy, 69 (2001) 59-74.
[53] M. Mehrotra, Solar Control Devices; Balance Between Thermal Performance and Daylight, in:Passive and Low Energy Cooling for the Built Environment, Santorini, Greece, (May 2005), pp. 991-996.
[54] S. H. Yoo, Manz, H, Available remodeling simulation for a BIPV as a shading device, Solar Energy Materials and Solar Cells, 95 (1) (2011) 394-397.
[55] E. Gratia, A. D. Herde, Are energy consumptions decreased with the addition of a double-skin?, Energy and Buildings, 39(5) (2007) 605-619.
[56] E. Gratia, De Herde, A, The most efficient position of shading devices in a double-skin facade, Energy Buildings, 39 (2007a) 364-373.
[57] D., Kim, Computational fluid dynamics assessment for the thermal performance of double-skin façades in office buildings under hot climatic condition. Building Services Engineering Research and Technology, 42 (2020) 014362442095296.
[58] Z. S. Zomorodian, M. Tahsildoost, Energy and carbon analysis of double skin façades in the hot and dry climate, Journal of Cleaner Production, 197 (2018) 85-96.
[59] M. Schaffer, L. Annabelle Bugenings , O. Kalyanova Larsen, C. Zhang, Exploring the potential of combining diffuse ceiling and double-skin facade for school renovations, Building and Environment, 235 (2023) 110199.
[60] D., Saelens, J. Carmeliet, H. Hens, Energy Performance Assessment of Multiple-Skin Facades, Hvac & Research, 9 (2003) 167-185.
[61] E. Sharifi, S. Lehmann, Comparative Analysis of Surface Urban Heat Island Effect in Central Sydney, Journal of Sustainable Development, 7(3) (2014) 23-34.
[62] M. Santamouris, Cooling the buildings - past, present and future, Energy and Buildings, 128 (2016) 617-638.
[63] R. Abdollahi Rizi, A. Eltaweel, A user detective adaptive facade towards improving visual and thermal comfort, Journal of Building Engineering, 33 (2021) 101554.
[64] M. S. Sadineni S , Boehm R, Passive building energy savings: A review of building envelope components, Renewable and Sustainable Energy Reviews, 15 (2011) 3617-3631.
[65] C., Lops, Double-Skin Façades for Building Retrofitting and Climate Change: A Case Study in Central Italy, Applied Sciences, 13 (2023) 7629.
[66] H. Radhi, S. Sharples, F. Fikiry, Will multi-facade systems reduce cooling energy in fully glazed buildings? A scoping study of UAE buildings, Energy & Buildings, 56 (2013) 179-188.
[67] N. Mingotti, T. Chenvidyakarn, Combined impacts of climate and wall insulation on the energy benefit of an extra layer of glazing in the facade, Energy and Buildings, 58 (2013) 237-249.
[68] A. Chan, C. TT, F. KF, L. Z, Investigation on energy performance of double skin façade in Hong Kong, Energy Build, 41(11) (2009) 1135-1142.
[69] A., Ahriz, The Use of Double-Skin Façades to Improve the Energy Consumption of High-Rise Office Buildings in a Mediterranean Climate (Csa), Sustainability, 14(10) (2022) 6004-6010.
[70] A. Tabadkani, S. Banihashemi, M. R. Hosseini Daylighting and visual comfort of oriental sun responsive skins: A parametric analysis, Building Simulation, 11 (2018) 663-676.

2383-8701/© 2024 The Author(s). Published by solarlits.com. This is an open access article under the CC BY license (https://creativecommons.org/licenses/by/4.0/).

[71] P. Tsikra, E. Andreou, Investigation of the Energy Saving Potential in Existing School Buildings in Greece. The role of Shading and Daylight Strategies in Visual Comfort and Energy Saving, Procedia Environmental Sciences, 38 (2017) 204 - 211.

[72] M., Alwetaishi, An investigation of shading devices in a hot region: A case study in a school building, Ain Shams Engineering Journal, 12(3) (2021) 3229-3239.

[73] S. Liu, K. Yu Ting, K.-L. L. Kevin , P. Wai Chan, E. Ng, Investigating the energy saving potential of applying shading panels on opaque façades: A case study for residential buildings in Hong Kong, Energy & Buildings, 193 (2019) 78-91.

[74] S. S. L. Yaghmaei, M. Khodagholi, Bioclimatic classification of Isfahan province using multivariate statistical methods, International Journal of Climatology, 29 (2009)1850-1861.

[75] N., Pirjalili, Criteria for designing educational buildings (architectural planning of primary and secondary schools), Technical and Supervision Deputy, 8 (2016) 1-12.

[76] T. Hong, J. Kim, J. Lee, C. Koo, H. S. Park, Assessment of Seasonal Energy Efficiency Strategies of a Double Skin Façade in a Monsoon Climate Region, energies, 6(9) (2013) 4352-4376.

[77] M. Ayoub, 100 Years of daylighting: A chronological review of daylight prediction and calculation methods, Solar Energy, 194 (2019) 360-390.

[78] D. H. W. L. Shuyang Li 1, Wenqiang Chen 2, Siwei Lou 3, Ernest K W Tsang Simple mathematical models to link climate-based daylight metrics with daylight factor metrics and daylighting design implications, Heliyon, 9(5) (2023) e15786.

2383-8701/© 2024 The Author(s). Published by solarlits.com. This is an open access article under the CC BY license (https://creativecommons.org/licenses/by/4.0/).